

Inhibition of on-chip PCR using PDMS–glass hybrid microfluidic chips

H. John Crabtree · Jana Lauzon · Yuen C. Morrissey · Brian J. Taylor ·
Tina Liang · Robert W. Johnstone · Alexander J. Stickel · Dammika P. Manage ·
Alexey Atrazhev · Christopher J. Backhouse · Linda M. Pilarski

Received: 24 November 2011 / Accepted: 13 March 2012 / Published online: 29 March 2012
© Springer-Verlag 2012

Abstract In the course of developing a microfluidic analytical platform incorporating the polymerase chain reaction (PCR) and subsequent capillary electrophoresis (CE) analysis for a variety of bio-assays, we examined PCR inhibition through surface interactions with the chip materials. Our devices perform PCR in a three-layer chip, a glass–poly(dimethylsiloxane)–glass sandwich in which the poly(dimethylsiloxane) (PDMS, a silicone rubber) layer is used for pneumatic membrane pumping and valving of the PCR reagents. Initial on-chip PCR–CE tests of BK virus replicated in multiple uncoated chips showed variable results, usually yielding no detectable product at the target sample concentrations used. Subsequent “chip-flush” experiments, where water or reagents were flushed through a chip and subsequently incorporated in off-chip PCR, highlighted bovine serum albumin (BSA) amongst other

pre-treatments, chip materials and PCR recipes as being effective in mitigating inhibition. When the BSA channel pre-coating was applied to on-chip PCR–CE experiments, a substantial improvement ($10\times$ to $40\times$) in signal-to-noise (S/N) of the CE product peak was conferred, and was shown with high confidence despite high S/N variability. This is the first study to quantitatively examine BSA’s ability to reduce inhibition of PCR performed on PDMS chips, and one of very few microfluidic PCR inhibition studies of any kind to use a large number of microfluidic chips (~ 400). The simplicity and effectiveness of our BSA coating suggest that passivating materials applied to microfluidic device channel networks may provide a viable pathway for development of bio-compatible devices with reduced complexity and cost.

1 Introduction

Publications regarding polymerase chain reaction (PCR) on microfluidic devices (Schneegaß and Köhler 2001; Zhang et al. 2006; Zhang and Xing 2007; Zhang and Ozdemir 2009) began to appear in the late 1990s (Kopp et al. 1998; Shoffner et al. 1996; Taylor et al. 1997; Waters et al. 1998; Wilding et al. 1995; Woolley et al. 1996), and those regarding PCR on microfluidic devices incorporating poly(dimethylsiloxane) (PDMS) around 2001. PDMS has many desirable attributes with regard to microfluidic devices such as flexibility, optical transmission and ease of fabrication, as demonstrated by numerous publications and several commercial products. Its use in membrane valves (as in this work) is an elegant exploitation of its mechanical flexibility (Grover et al. 2003; Unger et al. 2000). Regrettably, some of PDMS’ chemical attributes (e.g. porosity, chemical constituents and reactivity) may also render it

H. J. Crabtree · J. Lauzon · Y. C. Morrissey ·
B. J. Taylor · T. Liang · A. J. Stickel · D. P. Manage ·
A. Atrazhev · L. M. Pilarski (✉)
Department of Oncology, University of Alberta,
Edmonton, AB T6G 1Z2, Canada
e-mail: lpilarsk@ualberta.ca

R. W. Johnstone · C. J. Backhouse
Department of Electrical and Computer Engineering,
University of Alberta, Edmonton, AB T6G 1Z2, Canada

Present Address:
R. W. Johnstone
Teledyne Dalsa Semiconductor, 18 boul. de l’Aéroport,
Bromont, QC J2L 1S7, Canada

Present Address:
C. J. Backhouse
Department of Electrical and Computer Engineering,
University of Waterloo, 200 University Avenue West,
Waterloo, ON N2L 3G1, Canada

incompatible with certain samples and/or microfluidic operations such as PCR with which it comes into direct contact. Reduced size, diffusion lengths, and high surface area-to-volume ratios (SA:V) are some of the driving forces of microfluidic technology that make it enabling in many areas of analysis, but these may in fact be detrimental with a less inert device substrate like PDMS (Erill et al. 2003; Kricka and Wilding 2003). Miniaturisation in PDMS hybrid devices may exacerbate adsorption or absorption of analytes and/or reagents, or leaching of contaminants into the matrix. For reference purposes, the SA:V ratio for 25 μL in a typical conical microcentrifuge tube is 1.42/mm, while those seen in typical microfluidic channels 90 μm (as in this study) or 20 μm in depth are 34.5 and 139/mm, respectively.

The concepts of PDMS surface and bulk interactions as well as PCR fouling have separately been paid considerable attention in the literature, sometimes in the context of microfluidic devices. PDMS' porosity, by-products, potential to adsorb or absorb less polar or non-polar molecules, as well as need for (and methods of) surface treatment are relatively well known (Heo et al. 2007; Lee et al. 2003; Mehta et al. 2009; Ostuni et al. 2001; Rothka et al. 2011; Toepke and Beebe 2006; Wong and Ho 2009; Xia et al. 2007). Toepke and Beebe (2006) have shown that Nile Red and quinine dyes (molar masses of ~ 318 and ~ 324 g/mol, respectively) streamed through microfluidic channels are progressively absorbed into the surrounding PDMS bulk, easily reaching 100 μm from the channel wall (Toepke and Beebe 2006). Silicone rubber (of which PDMS is an example) has been shown to outgas a variety of low molecular weight compounds, such as short ($n < 10$) siloxane polymers and other organic compounds mostly arising from incomplete polymerisation, catalyst decomposition and by-products (Rothka et al. 2011). Lee et al. (2003) measured the relative affinity of a variety of organic solvents and water for PDMS by the extent to which they caused it to swell. They also found that strong organic solvents such as *n*-propanol and *n*-pentane would remove ~ 2.5 and 5 %, respectively, of the weight of a PDMS swatch immersed therein for 24 h, and suggested the extracted matter was uncross-linked oligomers. Multiple adsorbed and covalently bound surface treatments have been reported and are reviewed in the context of microfluidics by Wong and Ho (2009).

Studies regarding PCR fouling and its abatement have been performed off- and on-chip, sometimes with conflicting results. Bovine serum albumin (BSA) is an oft-used coating reagent to counter protein and cell adsorption on both hydrophilic and hydrophobic surfaces. Christensen et al. (2007) found that BSA coatings on silicon, glass and SU-8 test pieces inserted into the reaction mix of conventional

PCR (carried out in tubes) dramatically alleviated the PCR inhibition observed with the bare substrates. Kolari et al. (2008) also used small test pieces in PCR tubes, but found that neither BSA nor polyvinyl pyrrolidone (PVP) abated inhibition from them. Ostuni et al. (2001) coated BSA on the surface between the wells in a microwell array to inhibit cell adhesion. Using a silica-coated silicon microstructure, Taylor et al. (1997) found that PCR yield was dependent on BSA concentration, but at the right concentration yielded a twofold improvement. In contrast, Yu et al. (2007) found that dynamic coatings (added to PCR reagent mixture) of either BSA or polyethylene glycol (PEG) inhibited PCR in their PDMS microfluidic flow-through reactor. They also postulate, however, that the inhibition could stem from the static Tween 20 surfactant coating (applied prior to PCR). Quantitation and characterisation of *T.aq.* polymerase adsorption on different surfaces via contact angle, spectrophotometer and AFM measurements were performed by Prakash et al. (2007) using droplet-based microfluidics. They classified the 13 materials tested as having either contained or propagating adsorption based on whether a polymerase-laden droplet expanded with either a single or continuous decrease, respectively, in contact angle and polymerase concentration. Erill et al. (2003) also examined adsorption of *T.aq.* polymerase and DNA in silica-glass microfluidic chips and saw off-chip PCR efficiency decrease with the duration of polymerase (but not DNA) exposure to the chip. They also showed that BSA added to the reagent mixture effectively countervailed the loss of polymerase through competitive adsorption.

The Mathies group, pioneers in on-chip seamless PCR–capillary electrophoresis (PCR–CE) and whose chip architecture and valve designs are used in the present study, made use in their early work of two-layer, glass–glass chips with external pumps and valves coupled to the chip surface via multi-port manifolds (Lagally et al. 2000 2001a, b). They later designed three-layer, glass–PMDS–glass and four-layer, glass–PDMS–glass–glass valves for microfluidic chips that could be used alone, or in concert for pumping (Grover et al. 2003). In subsequent on-chip PCR work (Beyor et al. 2009; Lagally et al. 2004; Liu et al. 2006, 2007), they exclusively used the four-layer architecture (which nearly completely isolates the liquids in the PCR chamber and channel network from contact with the PDMS) for “improved chemical and biochemical compatibility” (Grover et al. 2003).

Our group has been working with on-chip PCR in hybrid glass–PDMS microfluidic chips (Kaigala et al. 2006, 2008, 2010) since 2006 and, in the process of scaling up chip fabrication to demonstrate chip-to-chip repeatability (Kaigala et al. 2006, 2008, 2010), we noted intermittent and sometimes prolonged periods where PCR amplification

failed or was unacceptably low. In many instances, poor performance was eventually traced to a component failure in an instrument or contaminated reagent, etc., but in others our suspicions turned to insufficiently controlled surface interactions inside the chip. Our experience, together with that of the researchers cited above, led us specifically to PDMS and its tendency to inhibit PCR in an environment with a high surface area-to-volume ratio.

In the present work, we examined the effects of BSA coatings along with a variety of other instrument, reagent and protocol choices for PCR in three-layer (glass/PDMS/glass) microfluidic chips with respect to their ability to enhance or hinder on-chip PCR. We also looked at potential fouling mechanisms that might be at play when PCR is performed in contact with PDMS. We evaluated several remedies in addition to BSA coating and carried out preliminary characterisation of failures.

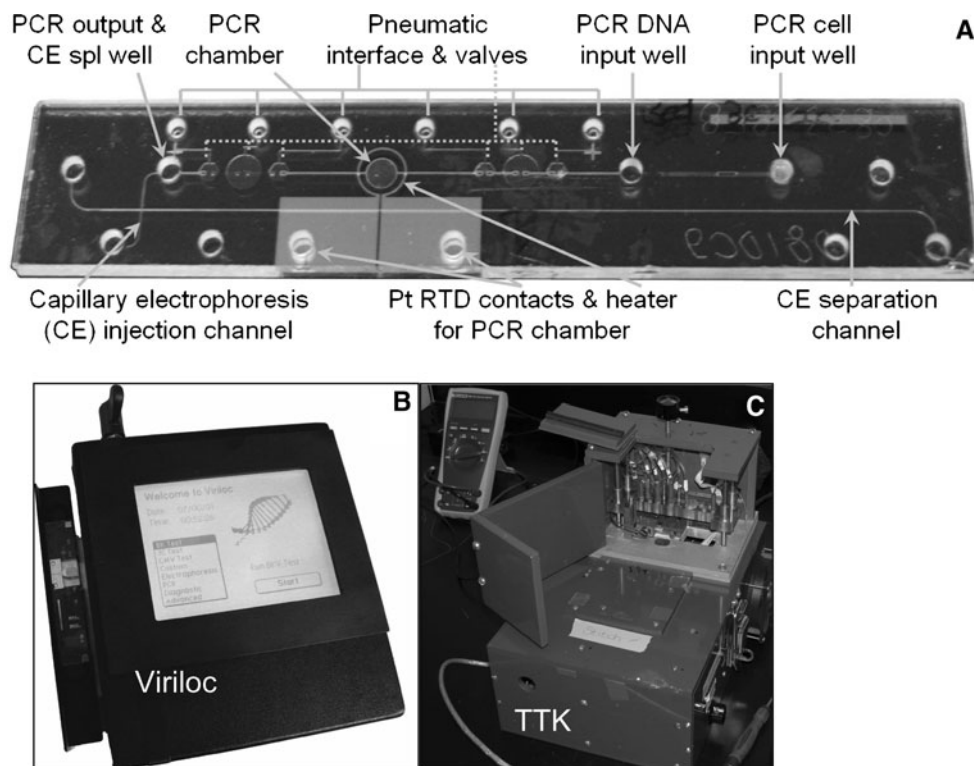
Our study complements previous studies examining the role of BSA in mitigating PCR inhibition in a microfluidic environment, but also differs from them in that we are measuring the enhancement conferred by a BSA coating to on-chip PCR for microfluidic devices that both incorporate PDMS and are in large number. It also differs from a number of studies which employ static or dynamic BSA (and other) coatings in microfluidic PCR devices made from a variety of materials, but which do not measure the effect of the coating (Bontoux et al. 2008; Hataoka et al. 2005; Oh et al. 2005; Trung et al. 2010; Xu et al. 2009; Zhang et al. 2010).

2 Experimental

2.1 Microfluidic chips

The microfluidic chips used in the study, depicted in Fig. 1a, are as described in our previous work (Kaigala et al. 2008). Briefly, they comprise three parts: a microfabricated glass top piece with a pneumatic channel network (for valve actuation), a PDMS layer and a microfabricated glass bottom piece with a fluidic channel network (for sample processing and analysis). The fluidic channel network was etched to a depth of 45 μm in the CE region, and 90 μm in the PCR region; channel widths were 110 and 200 μm , respectively, with corresponding SA:V of 34.5/mm in the PCR channels. The cylindrical PCR chamber was 90 μm deep and 3.1 mm in diameter (SA:V = 48.8/mm). The chips incorporate membrane valves whose design was inspired by the Mathies group (Grover et al. 2003). The microfabricated top and bottom pieces were made locally (University of Alberta Nanofab, Edmonton, AB, Canada). To prepare the PDMS membrane, we used a kit and mixed the elastomer and curing agent in a 7:1 volumetric ratio (Sylgard 184, Dow Corning, Midland, MI, USA) for 10 min at room temperature. Once combined, the mixture was degassed by vacuum until bubbles ceased to evolve (~ 5 min). PDMS membranes were poured in moulds that ensured the correct thickness of ~ 250 μm ; next, heat curing of membranes was achieved by placing the mould assembly in an oven at 80 $^{\circ}\text{C}$ which was

Fig. 1 Glass–PDMS–glass microfluidic chip and instruments for PCR–CE. Different functional areas and features on the microfluidic chip are shown in **a**, while the Viriloc and TTK are shown in **b** and **c**. Coordinated operation of the pneumatic membrane valves allowed PCR samples to be drawn from the PCR-in well into the PCR chamber and, after PCR, pumped to the PCR-out well. Electrophoretic separation was achieved by insertion of Pt electrodes in the four CE wells and execution of a simple HV programme. PCR thermal cycling was effected by a Peltier heater positioned below the PCR chamber in the Viriloc instrument, or by the onboard Pt RTD heater/sensor in the TTK instrument



allowed to cool overnight to room temperature. Pieces were cut from the cured membrane for individual chip bonding. In some cases as noted below, different types of commercially sourced 0.010 in.-thick PDMS sheets were used for the membranes (HT-6240, Bisco Silicones, Elk Grove, IL; NRV G/G 40D Silastic[®] silicone sheeting (biomedical grade, USP class VI designation), SMI, Saginaw, MI, USA). Chips were assembled by first subjecting the inner glass and PDMS surfaces to a 7-min ultraviolet–ozone treatment (Berdichevsky et al. 2004; Efimenko et al. 2002), bonding the PDMS layer to both glass layers and performing a pre-flush with SafetyCoat (4017-01, JT Baker, Phillipsburg, NJ, USA) solution through the PCR chamber and valve network to keep the latter from sticking.

As shown in Fig. 1a, the chip has a sample preparation region (not used in this study), a PCR region and a CE region. The glass–PDMS–glass design allows the flexible PDMS membrane to be used as a (normally closed) valve that is actuated with vacuum to open and pressure to close. The three valves on either side of the PCR chamber are operated in concert to create a pump that draws liquid from the PCR-in well to the PCR chamber and later on to the PCR-out/CE-in well.

After experiments were performed on three-layer chips, the chips were recycled by dissolving the PDMS membrane in the following manner. First, the entire chip was immersed in Dynasolve, a relatively non-polar solvent (Dynasolve 210, dichloromethane and dodecylbenzenesulphonic acid in a ~3:1 mass ratio, Dynaloy, Indianapolis, IN, USA) for a 48-h soak to degrade the PDMS membrane and free the two glass pieces. After removal from Dynasolve, the glass pieces were washed in 70 % (vol) isopropanol, wiped dry and put through an acid piranha wash (3:1 volumetric ratio of concentrated H₂SO₄ and H₂O₂). Last, the glass pieces were placed in an oven, annealed at 400 °C for 2 h and allowed to cool overnight to room temperature prior to re-use. Top and bottom glass pieces were engraved with identification tags to track performance of individual glass pieces once reassembled.

The all-glass chips (SC, Micralyne) for some chip-flush experiments have a two-intersecting channel layout and are described in detail elsewhere (Crabtree et al. 2001).

2.2 Instrumentation

Two versions of instruments, both designed to operate these chips, were used in our experiments and are shown in Fig. 1b, c. Both systems nominally perform the same functions of (1) pressure- and vacuum actuation of the valves around the PCR chamber, (2) thermal cycling of the PCR chamber, (3) application of a high-voltage programme to the CE channel network to effect the separation of fluorescently labelled DNA amplicons, and (4) detecting the DNA via laser-induced fluorescence (LIF) in the

separation channel. The first, termed a “Tricorder Tool Kit” (TTK), was developed in previous research and is described in detail elsewhere (Kaigala et al. 2010); of note, the TTK uses an integrated Pt RTD heater/sensor (Hoang et al. 2008) on the chip to perform the thermal cycling. The second instrument, termed a Viriloc, uses a Peltier heater/cooler to perform thermal cycling. In practice, after PCR was performed on either of the first two instruments, a third commercial instrument, the μ TK or Microfluidic Tool Kit [Micralyne, Edmonton, AB, Canada; described elsewhere (Crabtree et al. 2001)] was used to perform CE with LIF detection on a second identical microfluidic chip due to complications in effecting a truly seamless PCR–CE operation with either TTK or Viriloc instrument, given the present chip design. LIF data were collected at 200 Hz and exported as a text file. Data used for illustrative purposes in Figs. 3, 4 and 5 were smoothed with a 51-point boxcar filter in Igor Pro v. 3.14 (WaveMetrics Inc., Lake Oswego, OR, USA) for visual clarity, especially for weak peaks seen in runs with chip-flushed water, or without BSA coating.

PCR for off-chip positive control samples was performed on a conventional thermocycler (GeneAmp 9700, Applied Biosystems, Pleasanton, CA, USA).

2.3 Reagents

25 μ L PCR reagent mixtures were prepared daily per Table 1, with slight recipe modifications made for later on-chip experiments to optimise performance. Primer sequences have been published previously (Manage et al. 2011). Tris-TAPS-EDTA (or TTE) buffer was made up at the 10 \times concentration (500 mM in both tris(hydroxymethyl)amino-methane (tris; Fisher Scientific) and *N*-(tris(hydroxymethyl)methyl)-3-aminopropanesulphonic acid (TAPS; Sigma), 10 mM in disodium ethylenediaminetetraacetate (EDTA; Sigma)) and diluted with autoclaved deionised water as required. BK virus (BKV) template was provided by the Alberta Provincial Laboratories for Public Health (Edmonton, Canada) and was confirmed by LightCyclerTM analysis to have a titre of 6×10^9 copies/mL. For on-chip PCR, each well received ~360,000 copies of BKV template of which ~80,000 occupied the 661 nL PCR chamber prior to amplification. PCR amplicons (295 bp in length) were also confirmed by DNA sequencing. Other reagents used for chip-flush experiments included polyethylene glycol (PEG, Sigma Aldrich), polyvinylpyrrolidone (PVP, Sigma-Aldrich) and *n*-pentane (Caledon Laboratories).

2.4 Procedure: chip-flush (on-chip flush, off-chip PCR, on-chip CE)

For a given “chip-flush” experiment, water or selected PCR reagents were loaded into the chip’s PCR-in well

Table 1 Reagents used for PCR reagent mixture

Reagent	Vol. (μL)		Source
	Off-chip	On-chip	
10X PCR buffer (200 mM Tris–HCl, 500 mM KCl; pH 8.4)	2.5		Invitrogen 10966-034
10 μM 5' BKV 25b forward primer	Unlabelled (off-chip)	–	IDT 37822830 (off-chip)
	Alexafluor 647 (on-chip)	–	IDT 44457126 (on-chip)
10 μM 3' BKV 26b reverse primer	Cy5 (off-chip)	–	IDT 39804571 (off-chip)
	Alexafluor 647 (on-chip)	–	IDT 45215441 (on-chip)
10 mM dNTPs	0.5		Invitrogen 10297-018
50 mM MgCl_2 (4 mM final concentration)	2.0		Invitrogen 10966-034
5 U/ μL Platinum® <i>T.aq.</i> polymerase	0.5		Invitrogen 10966-034
BKV template, 6×10^9 copies/mL	0.5		Provincial Laboratory of Alberta
1 % BSA (from 2% stock)	0.5		Sigma
DMSO (4% at final concentration)	1.0		Fisher
H_2O , PCR grade	16.25	16.5	MP Biomedicals 821739
Total	25		

The mixture was modified slightly for on-chip studies in an ongoing effort to improve PCR yield

(Fig. 1a) and subsequently pumped (via onboard pumping) through the PCR channel network to the PCR-out well; the coatings applied to the chips and reagents flushed varied as described in the results and discussion. Chips were at room temperature during the procedure, and flush duration was ~ 1 – 2 min, as required to add reagents, pump and remove the reagents, with no intentional residence time of the reagents in the PCR channel network. The flushed reagents were recovered, substituted for like reagents in the reagent mix and tested with off-chip PCR to evaluate their efficacy after exposure to the chip channel network. The thermal cycling programmes used for on- or off-chip PCR are shown in Table 2. On-chip CE analysis was used to evaluate the effect of the chip-flush.

2.5 Procedure: on-chip PCR–CE and controls (on-chip PCR, on-chip CE)

A BSA pre-coated chip was prepared by flushing a 1 % BSA solution through the assembled chip's PCR valves and chamber (termed coated chip); once the solution had permeated the PCR section of the chip, it was left for a soak time (1 h unless otherwise indicated) for thorough

coating. The PCR channel network was then flushed with PCR reagent mix as it was pumped in from the PCR-in well using on-chip pumping. Uncoated chips merely had PCR reagent mix pumped in as the initial step. The PCR-in well was then flushed with water, and PCR thermal cycling was initiated via the instrument's control software per Table 2.

The PCR chamber liquid was then pumped out to the PCR-out/CE-in well by filling the PCR-in well with $0.1 \times$ TTE and pumping to displace the PCR product from the reaction chamber to the PCR-out well. This PCR product solution was used directly, or diluted as either dilution 1 or 2: 0.3 μL of product solution was added to 3 μL of $0.1 \times$ or $0.01 \times$ TTE, respectively; 3 μL of product solution or 3.3 μL of dilution 1 or 2 was pipetted back onto a second three-layer chip for the CE analysis. The voltage programme was 300 V across the short injection channel (9.64-mm long) for 60 or 90 s to inject the sample and 600 V across the long separation channel (90.33-mm long) for ~ 200 s to separate the fluorescently labelled DNA amplicons present. LIF detection occurred at ~ 13 mm from the channel intersection, just before the Pt heater contact pad.

Table 2 Thermal cycle programmes for PCR

Stage	Thermocycler		Viriloc-1: 3-step		Viriloc-1: 2-step		TTK-S: 3-step	
	Temperature ($^{\circ}\text{C}$)	Time (s)	Temperature ($^{\circ}\text{C}$)	Time (s)	Temperature ($^{\circ}\text{C}$)	Time (s)	Temperature ($^{\circ}\text{C}$)	Time (s)
Pre-melt	94	120	94	120	94	120	94	120
Thermal cycling (35 cycles)	94	20	94	30	94	15	94	10
	60	30	57	30	60	30	58	20
	72	30	72	30			70	20
Post-extension	72	120	72	120	73	60	70	120

Slightly different programme variations are seen in the set points and step durations due to different heating characteristics of the different systems

Off-chip thermocycler positive control PCRs were run with 10 μL of reagent mix and were subsequently evaluated by CE on the μTK system in the same manner as on-chip products.

2.6 Data analysis for signal-to-noise (S/N) measurements

To provide some degree of quantitation for the influence of different instrumentation, reagents and protocols on the PCR, the size of each product peak was determined in terms of its signal-to-noise ratio. Given (1) the asymmetric (tailing) nature of both the primer and product peaks, (2) the truncation of some product peaks by the data acquisition hardware due to the high sensitivity setting for the photomultiplier tube (PMT), discussed below and (3) the fact that the product peak lay on the decaying tail of primer peak, computational analysis was required to measure peak heights consistently and ensure that the sloping baseline did not inflate the estimate of baseline noise.

Product peak quantitation is illustrated in Fig. 2 and described in detail in Appendix 1. S/N of the PCR product peak in the electropherogram (Fig. 2a) was calculated as peak height/baseline noise. Baseline noise was evaluated from 5–7 s before the peak maximum, on the decaying primer peak tail (Fig. 2b). In the case of truncated peaks, the estimated true peak maximum was calculated as a fraction of the height of the intersection of linear extrapolations of a peak's front and tail (Fig. 2c). To ensure that the slope of the baseline, which varied from run to run, did not influence the noise calculation, this 2-s segment was regressed, and the slope removed prior to calculating the magnitude of the noise (Fig. 2d).

Once S/N ratios were established for each run, runs were grouped by experiment into 'data groups', and averages and standard deviations were calculated for each group. For subsequent comparison of pairs of data groups to highlight the effectiveness of a given procedure (or lack thereof), and in light of the high variability seen with most data groups, an unbiased statistical approach that accommodated small, unequal sample sizes and unequal variances for the two groups in question was used; the specifics of the statistical analysis are provided in Appendix 2.

3 Results and discussion

3.1 On-chip flush, off-chip PCR and on-chip CE

In our initial consideration of pernicious inner chip surface interactions with the PCR reagents, we formed theories for mechanisms and possible remedies. Akin to others cited in the Sect. 1, we postulated that the bare PDMS might inhibit

PCR by (1) adsorption and/or absorption of one or several PCR reagents, most notably the *T.aq.* polymerase enzyme or (2) infusion of various leachates into the aqueous PCR reagent mix. We next mapped out a matrix of "chip-flush" experiments wherein certain reagents (usually the water, and sometimes the entire reagent mix) were pumped through the chip's PCR channel network via its onboard pumps and then used for off-chip thermocycler PCR with subsequent on-chip CE analysis to evaluate inhibitory effects.

A typical example of PCR inhibition is shown in Fig. 3. Here, $\sim 70 \mu\text{L}$ of clean water was pumped through a bare (non-BSA-coated) chip and subsequently used to substitute none, 1, 2, 4 and 8 μL , or all of the clean water in the reagent mix (Table 1) for off-chip (thermocycler) PCR; subsequent on-chip CE was used to evaluate the results. Initially, with no chip-flushed water, the electropherogram is fairly clean, with strong, off-scale peaks for both the primer and product at ~ 85 and ~ 120 s, respectively, and a small peak from an unidentified product at ~ 100 s. As the proportion of chip-flushed water increased, several features in the electropherogram changed: (a) three shorter fragment peaks between the primer and product peak first appeared and then increased in magnitude; (b) the unidentified product peak at 100 s increased in magnitude; (c) the magnitude of the primer and correct product peaks diminished to nearly zero; and (d) the magnitude of the other fragment peaks reached a maximum at 1/8 flushed water and decreased for higher flushed water concentrations. Our interpretation of these flushed water-induced electropherogram anomalies includes a number of possible pathways (Chou et al. 1992; D'Aquila et al. 1991; Wilson 1997), all of which assume reagent fouling via leachates in the flushed water: (a) mis-priming during PCR leading to different fragments, longer and shorter than the product, being formed; (b) formation of primer *n*-mers, which may generate the peaks migrating earlier than the product; and (c) reduction in the activity of the *T.aq.* polymerase enzyme, leading to decreasing product peak size.

A variety of other chip-flush experiments with off-chip thermocycler PCR and subsequent on-chip CE was performed to try to either improve poor and/or highly variable output (qualitatively estimated by the presence and magnitude of the PCR product peak in the electropherogram), or to correlate changes in PCR output and presence of non-specific peaks to a mechanism. These experiments are summarised in Table 3, and some examples of electropherograms showing non-specific peaks arising from PCR mix flushed through glass chips as well as the effect of BSA pre-coating on water flushed through a three-layer chip are presented in Fig. 4. Some experiments showed trends, while others showed irreproducible results. In all cases, the electropherogram for off-chip PCR positive

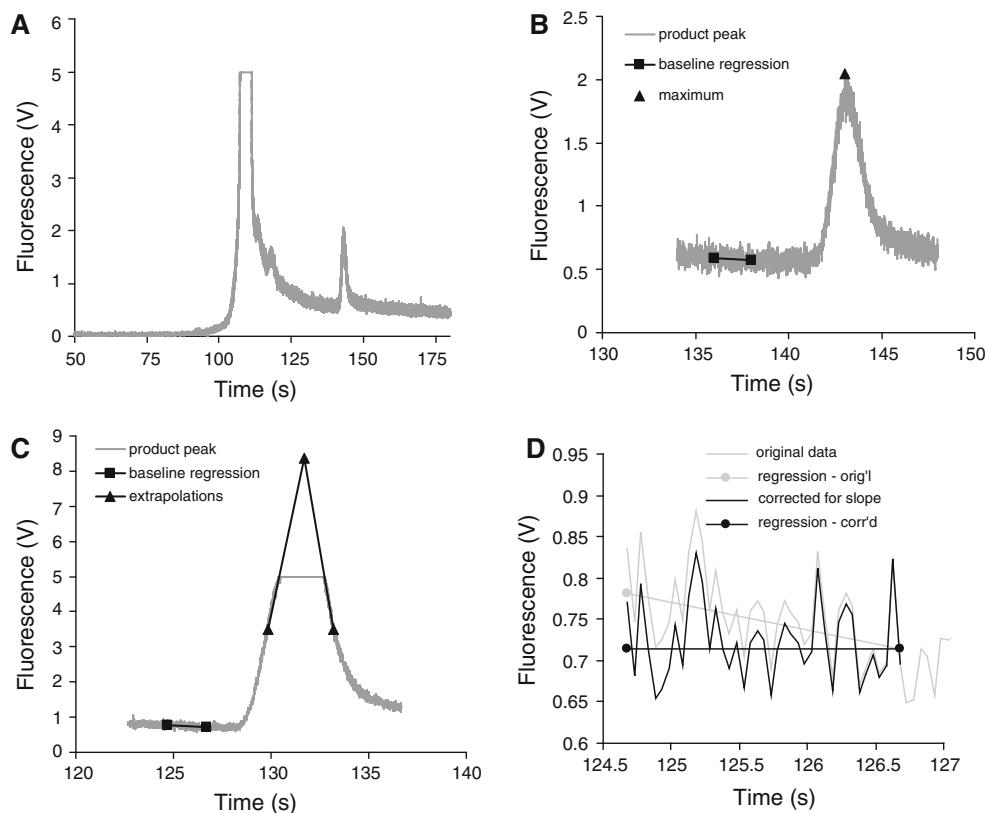


Fig. 2 Typical electropherograms for on-chip PCR and details concerning graphical analysis for S/N values of the product peak. Full electropherogram is shown in **a**, while only the section near the on-scale product peak is shown in **b**; both the regressed baseline and peak maximum used for S/N calculations as described in the text are *highlighted* in **b**. An example of an off-scale product peak is shown in **c**; here the regressed baseline and peak front and tail extrapolations used to estimate the interpolated peak maximum are *highlighted in black*. To remove the bias imparted by the sloping baseline (**b**, **c**)

the measurement of baseline noise, baselines were regressed in this 2 s segment and had the slope removed. The 2 s regressed baseline segment from **c** is shown in **d**; the data trace and linear regression line for the downward decaying original data are shown in *grey*, while those for the data corrected for slope are shown in *black*. The corrected data were used to estimate baseline average and standard deviation values. For clarity, every 10th point is shown in plot **d**. More details can be found in Appendix 1

controls (with no chip-flush components) were similar to Fig. 3a. These experiments were designed to highlight conditions that would produce a clean off-chip PCR, namely one with a strong product peak and no non-specific peaks, even after high surface-area-to-volume ratio contact with the chip inner surfaces. Only two chip-flush experiments, #7 (chip with *n*-pentane-soaked PDMS) and #8 (chip with BSA pre-soak; Fig. 4b), generated both strong product peak and near absence of non-specific peaks, suggesting the potential to abate on-chip surface interactions. Based on this, on-chip PCR was performed in likewise prepared chips. Chips with *n*-pentane-soaked PDMS membranes were not able to generate a PCR product, while those having had the PCR channel network pre-soaked with BSA did; subsequent experimentation with BSA pre-soaking is described in the next section.

Clear attribution of root causes, such as the presence of PDMS leachates and subsequent fouling of polymerase function or primer binding, or loss of polymerase (or other

reagents) to absorption or adsorption in the PDMS, cannot be made in a rigorous manner based on our findings alone. However, some mechanisms and observations do come to the fore. The fact that water was the only chip-flushed reagent used in the subsequent off-chip PCR shown in Fig. 3 suggests a leachate-fouling mechanism. As mentioned previously, Whitesides' group showed significant extraction of uncross-linked oligomers with strong organic solvents such as *n*-pentane (Lee et al. 2003). Though unknown, the extent to which this extraction is at play during on-chip PCR with our PCR reagent mixture in a micro environment bears consideration. It may be that extraction is behind the effectiveness of *n*-pentane as a pre-soaking reagent. The fact that PCR reagent mix that was flushed through all-glass chips generated non-specific peaks with a very strong product peak in subsequent off-chip PCR/on-chip CE suggests that some degree of polymerase fouling may occur via transient adsorption (Erill et al. 2003; Prakash et al. 2007) to the glass walls. It

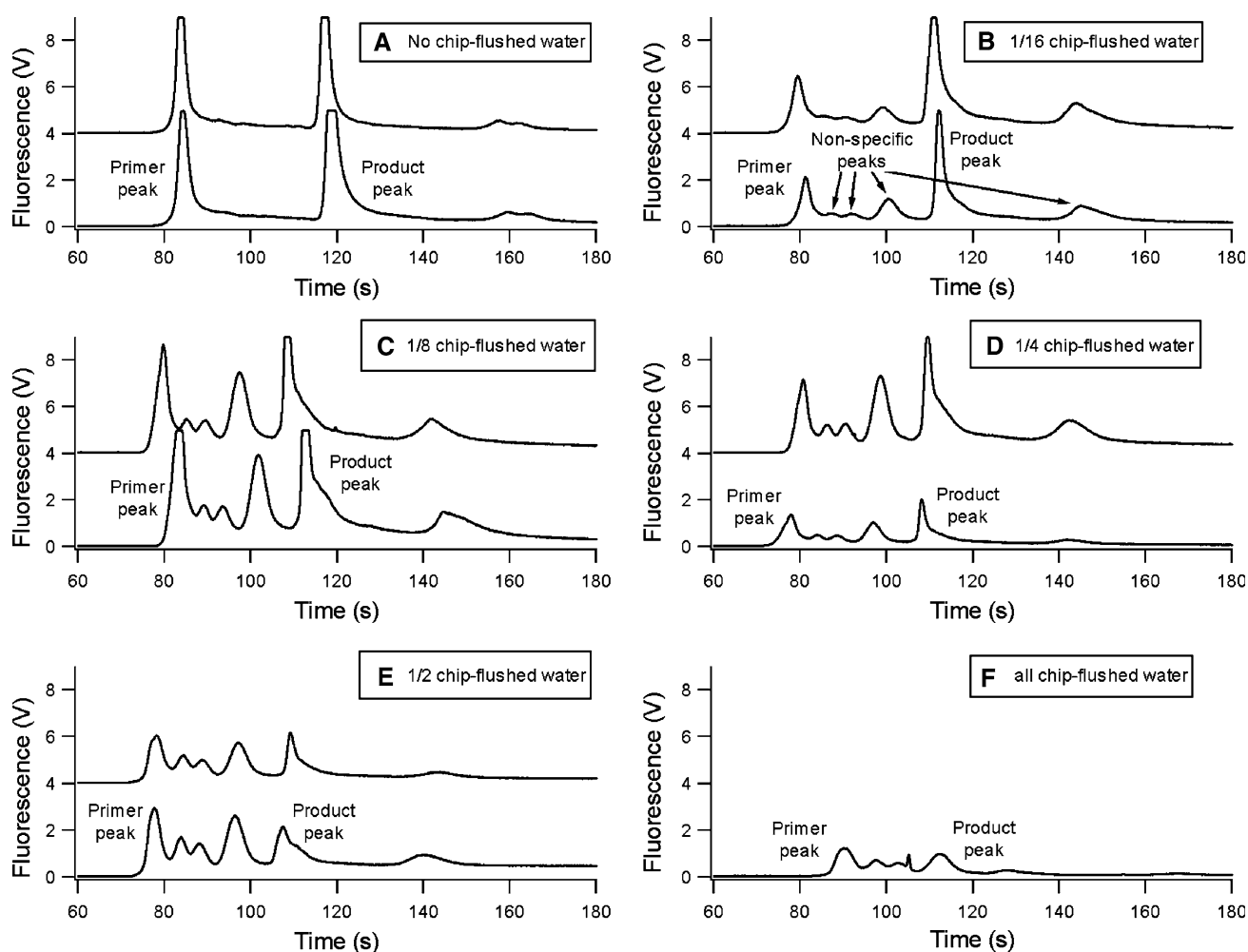


Fig. 3 Off-chip PCR with varying amounts of water flushed through uncoated chips. Duplicate electropherograms of off-chip PCR products with varying amounts of water that has been flushed through uncoated chips included in the PCR mixture. Plots **a** through **f** show the gradual progression from clean electropherogram with no chip-

flushed (contaminated) water to **f** with only chip-flushed water. Plot **a** represents the appearance of a typical off-chip control PCR electropherogram. Electrophoretic separations were performed on-chip and have been smoothed for clarity

may be that different mechanisms (e.g. PDMS leachate fouling, polymerase adsorption on a glass or PDMS channel surface) can produce similar effects on the PCR to different extents, and that the severity of the effects is a function of residence time and temperature, both of which are different in a chip-flush experiment versus on-chip PCR. In flow-through studies performed by Gonzalez et al. (2007), no relationship between PCR yield and residence time was found; however, they used large diameter tubing (0.5-mm diameter; SA:V = 8/mm, ~4 times lower than in this study) and they did not test PDMS.

3.2 BSA enhancement of on-chip PCR output

Based on the ability of a BSA coating to suppress the inhibition normally seen when incorporating chip-flushed water in off-chip PCR as described in the previous section,

we tested the effect of BSA pre-soaks for on-chip PCR. The ability of BSA to suppress on-chip PCR inhibition is shown in Fig. 5, a comparison of typical results from uncoated and BSA-coated chips. Chips that were given a 1-h BSA pre-coat (upper grey trace) showed very strong product peaks, whereas chips that were not pre-coated with BSA showed either a minuscule product peak (lower black trace) or none at all in many instances. The PMT sensitivity was maximised to detect any product that was amplified in uncoated chips. It is also worth noting that the migration times for the primer and product peaks can be seen to shift somewhat in the two traces of Fig. 5, as well as in Figs. 2, 3 and 4b. This run-to-run variability is due to chip-to-chip differences in the polyacrylamide gel that is inserted in the CE channel network of the chips.

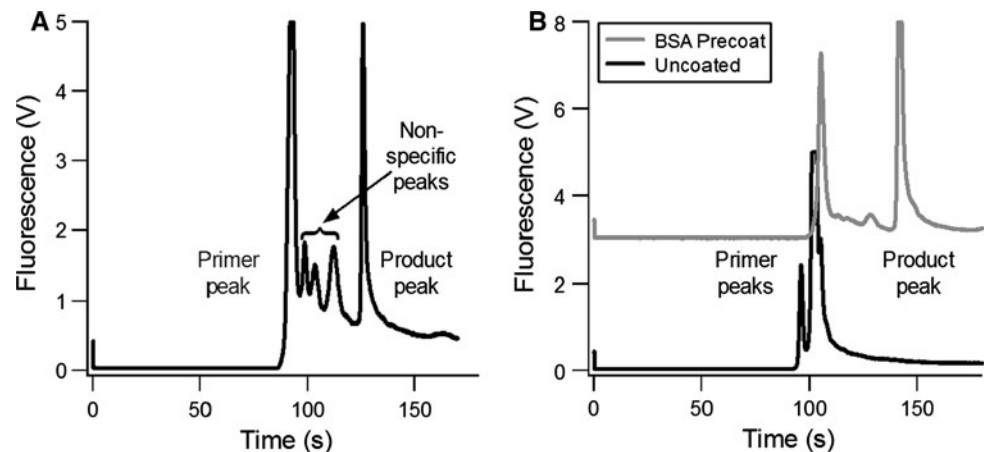
The difference between PCR product generated in BSA-coated and uncoated chips shown in Fig. 5 is both striking

Table 3 Off-chip PCR ‘chip-flush’ experiments

Experiment				Electropherogram	
#	Chip-flushed component	Off-chip PCR additive	Chip details	Product peak	Non-specific peaks
1	PCR mix	–	Two-layer, all-glass chips	Strong	Strong
2	PCR mix	1 or 0.1 % BSA	–	Weak	Strong
3	Water	1 or 2 % PVP	–	Weak	Strong
4	Water	1 or 2 % PEG	–	Strong	Strong
5	Water	–	Different kinds of PDMS: in-house; 7:1 and 10:1 volumetric ratio of elastomer:curing agent 2 externally sourced	Irreproducible (strong and weak)	Strong
6	Water	–	PDMS membrane soaked in boiling water for 1 and 4 h	Irreproducible (strong and weak)	Strong
7	Water	–	PDMS membrane soaked in <i>n</i> -pentane for 72 h	Strong	Very weak
8	Water	–	PCR channel network pre-soaked with 1 % BSA for 1 h	Strong	Very weak

To find conditions that would minimise on-chip PCR inhibition, different PCR components were flushed through a chip and included, possibly with additives, in the reagent mix for thermocycler PCR. Uncoated three-layer glass–PDMS–glass chips were used unless otherwise specified under the ‘Chip details’ column. The products were analysed by subsequent on-chip CE, with product and other peak characteristics as noted in the table under the Electropherogram columns. Only two experiments, #1 (glass chip) and #4 (PEG coating), were able to strongly enhance the product peak size, but still did not reduce the presence of non-specific peaks. Two other experiments, #7 (*n*-pentane pre-soak) and #8 (BSA pre-soak), showed potential for abating surface interactions by virtue of the strong product peak and near absence of non-specific peaks

Fig. 4 Off-chip PCR with **a** PCR mix flushed through glass/glass chips and **b** water flushed through BSA-coated and uncoated glass/PMDS/glass chips (Table 3, experiments 1 and 8, respectively). Electrophoretic separations were performed on-chip and have been smoothed for clarity



and reproducible, though quantifying the reproducibility is challenging. Many experimental steps involved in performing a PCR–CE run are manually performed, which introduces a degree of variability in the quantitative result. Such steps include fabricating the chips, applying coatings, pumping nominally reproducible volumes of PCR reagents in and product out of the PCR channel network, reaction efficiency during PCR, electrophoretically injecting the PCR product into the CE channel network and collecting the LIF signal for the electropherogram. Reaction efficiency is a particularly important factor to consider, since it can be influenced by many factors (thermal control and contact, small variations in reagent stoichiometry, etc.), and since it has a power function influence (e.g. x^{35} , where x approaches 2 depending on efficiency, and 35 is the

number of PCR thermal cycles) on the final quantity of product generated. The sum of this variability manifested itself in the signal strengths seen for both uncoated and coated chips. To demonstrate the effectiveness and reproducibility of BSA coatings as well as optimise product signal strength, a large matrix of experiments, involving hundreds of three-layer chips, was designed and executed.

In conventional real-time PCR, reaction output and starting quantity are quantitated by monitoring DNA product fluorescence at each chain extension step during the reaction to generate a sigmoid amplification curve. Quantitation is achieved by determining the cycle at which the exponential reaction is maximised, C_p , which is a function of starting sample concentration and other factors that affect reaction efficiency (Atrazhev et al. 2010).

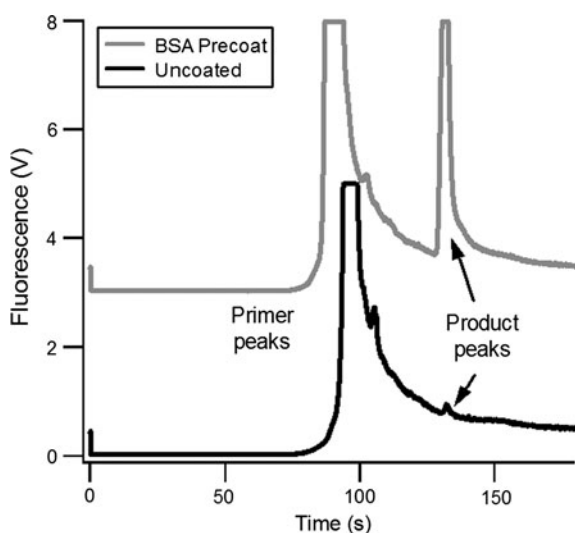


Fig. 5 Typical electropherograms from on-chip PCR–CE using uncoated and BSA-coated chips. The product peaks from PCR run on coated chips are usually easily visible, while those run on uncoated chips are weak or undetectable. Experimental conditions: CE sample was 0.3 μL PCR output liquid added to 3 μL of 0.1 \times TTE buffer (dilution 1) and was injected for 90 s for plug formation; 60 min BSA pre-coat for upper trace; 3-step PCR performed on Viriloc-1

Quantitation of the reaction at the end point is not ideal (Fraga et al. 2008; Valasek and Repa 2005). The rate of reaction and amount of product produced in PCR are both dependent on several factors such as the availability of reagents that get consumed, e.g. primer and dNTPs, the concentration and activity of enzymes and cofactors that catalyse the reaction and do not get consumed, e.g. polymerase and Mg^{2+} . Importantly, thermal degradation of the polymerase activity results in considerable variability in reaction rate and end point product concentration. As a result of all of these contributing factors, end-point concentration is more variable and less ideal for quantification than that measured in the exponential phase in real-time PCR. Unfortunately, it was not possible with our experimental apparatus to measure fluorescence during the course of the reaction, so the height of the product peak in the electropherogram, quantified by its S/N measurement (described in detail in Sect. 2; Appendix 1) was chosen instead as the comparative figure of merit to reflect PCR output for different experiments (end-point quantitation).

The conscious choice of maximising LIF detector sensitivity at the expense of dynamic range was made, and as a result many product peaks from successful PCR runs on BSA-coated chips were “clipped” at the detector’s maximum of 5 V, e.g. Figs. 4 and 5. The maximum for a clipped peak was estimated via interpolation methods (see Sect. 2; Appendix 1).

The effect of BSA pre-soaks and other experimental conditions on PCR output are shown in Table 4. The PCR

output is reported as peak S/N. Results are segregated into data groups along several differences in instruments, reagents and protocols, as shown in the column headers for instrument, number of PCR steps (3 or 2), BSA pre-soak time, and CE sample composition and injection time for plug formation (the latter refers to time allowed for all sample components to reach the channel intersection prior to being injected and analysed in the long separation channel; details pertaining to this consideration can be found elsewhere (Footz et al. 2001; Pilarski et al. 2005)). Each discrete run ID entry represents a single on-chip PCR experiment on a fresh chip; though the PCR product from a given chip was often used in multiple electrophoretic separations, only one is shown per on-chip PCR to ensure proper weighting in the statistical values.

Table 4 represents a subset of all the data gathered by our group for which several experimental conditions such as evolving PCR recipes, thermal cycle settings and first run of n CE replicates were precisely consistent. This selected subset comprises 69 from a total of ~ 400 independent chip runs, with CE replicates bringing the total number of electropherograms individually analysed to $\sim 1,000$. While automated future versions will be less labour intensive, at present a run requires a full day if PDMS membrane preparation, chip assembly, instrument calibration, on-chip PCR and CE, chip rejuvenation and preliminary data analysis are considered. While it is important to provide the full data set, only two observations can easily be made directly from this table. The first is that, for almost all data groups, the variability in the S/N values is relatively high, as shown by standard deviations that are usually more than half of the average for a given group; this is in large part a result of the use of the end-point quantitation method, as described above. The second is that, despite this high variability, PCR performed on BSA pre-soaked chips is shown to be far more effective than on uncoated chips (S/N of 47 vs. 1.2, 88 vs. 9, and 114 vs. 5 for data groups C vs. A, D vs. B, and G vs. F, respectively).

To ensure that the comparison of any pair of data groups pertaining to different experimental approaches was unbiased and properly weighted, particularly in light of the small sample sizes and high variability in S/N values, the statistical approach for comparing averages described in Sect. 2 and Appendix 2 was used. Table 5 shows a summary of comparisons with the merit of each quantified by the confidence level at which the average S/N values for each data group can be considered distinct.

Several conclusions can be drawn from Table 5. Comparison 1 between BSA-coated and uncoated chips shows that the BSA coating significantly improves the S/N. Comparison 2 shows that two- and three-step PCR both worked relatively well and were not significantly different

Table 4 Effect of various instruments, reagents and protocols used for on-chip PCR on the signal-to-noise ratio of the product peak in subsequent CE

Instrument	PCR steps	BSA pre-soak of channel network	CE sample injection time/ preparation	Run ID	S/N: discrete	S/N: average ± 1σ	Data group			
Viriloc-1	3	None	60 s/direct from PCR	18	ND	1.2 ± 2.7	A			
				19	ND					
				20	ND					
				22	ND					
				21	6.0					
		90 s/direct from PCR	69	ND	8.8 ± 10.9	B				
			76	5.4						
			65	21.1						
			13	11.0						
			8	15.0						
		60 min	60 s/direct from PCR	5	17.5	47.4 ± 42.5	C			
				6	23.0					
				14	28.2					
				4	32.3					
				17	34.0					
	15			37.0						
	16			40.5						
	3			44.4						
	11			51.2						
	12			73.7						
	9			~79 (>76.8)						
	10			~178 (>93.8)						
	2			90 s/direct from PCR	68			21.3	88.0 ± 56.6	D
					75			60.4		
					78			~78 (>47.8)		
		70	~108 (>91.0)							
		64	~172 (>95.2)							
		49	5.3							
		54	18.1							
		51	22.0							
55		29.7								
50		32.7								
59		57.7								
61		82.6								
52		85.8								
53		115.4								
60		~150 (>104.5)								
3	None	90 s/dilution 1	32	4.5	5.0 ± 0.6	F				
			41	5.4						
	60 min	90 s/dilution 1	33	83.1	113.8 ± 43.3	G				
			43	144.4						
	10 min	90 s/direct from PCR	79	6.2	75.3 ± 49.5	H				
			67	51.7						
			74	75.5						
			63	~112 (>74.8)						
	Just prior to PCR	90 s/direct from PCR	71	~131 (>84.3)	55.0 ± 31.9	I				
			66	10.3						
73			61.1							
62			62.2							
3	60 min	60 s/direct from PCR	77	86.1	16.9 ± 12.9	J				
			25	ND						
			26	13.0						
			37	13.6						
			40	22.9						
		90 s/direct from PCR	29	34.8	94.8 ± 10.2	K				
			47	~88 (>41.8)						
		60 s/dilution 1	44	~102 (>78.6)	56.9 ± 34.2	L				
			36	12.1						
			31	38.7						
			39	51.6						
			28	88.8						
		90 s/dilution 1	24	93.0	80.9 ± 33.1	M				
			45	57.5						
			46	~104 (>86.7)						
60 s/dilution 2	35	13.6	67.4 ± 46.4	N						
	38	29.1								
	27	72.9								
	23	95.6								
	30	~126 (>75.6)								

In all cases, PCR was performed on three-layer, glass–PDMS–glass chips. For CE sample preparation, “direct from PCR” means that ~3–4 μL of product from the PCR-out well was pipetted directly into the PCR-in well of the CE chip (different chip used as discussed in text). For dilutions 1 and 2, 0.3 μL of product was added to 3 μL of 0.1× or 0.01× TTE, respectively, and pipetted into the PCR-in well. Discrete S/N values stated as “~aaa (>bb.b)” refer to the S/N ratios obtained by graphical extrapolation (~aaa value) or using the maximum value of the clipped peak (>bb.b value); see Appendix 1 for more details. Subsequent statistical calculations used extrapolated S/N values and 0 for non-detectable (ND) entries

Table 5 Comparison of specific experimental parameters from Table 4 to determine relevance

Comparison					Confidence level for distinction (%)
#	Description	Detail	Other conditions	Data groups	
1	BSA pre-soak	60 min versus none	60 s direct inj.	C versus A	99.8
			90 s direct inj.	D versus B	95
			90 s dil. 1 inj.	G versus F	80
2	PCR steps	3- versus 2-step cycle		D versus E	60
3	CE sample injection time	90 s versus 60 s injection plug formation	V-1; direct inj.	D versus C	70
			TTK-S; dir. inj.	K versus J	98
			TTK-S; dil. 1 inj.	M versus L	<50
4a	CE sample preparation	Dil. 1 versus dir. inj. Dil. 2 versus dir. inj. Dil. 2 versus 1	TTK-S; 60 s inj.	L versus J	90
				N versus J	90
				N versus L	<50
4b		Dil. 1 versus dir. inj.	V-1; 90 s inj.	G versus D	<50
			TTK-S; 90 s inj.	M versus K	<50
5a	BSA pre-soak time	60 min. versus none 10 min versus none fleeting versus none	V-1; 90 s direct inj.	D versus B	95
				H versus B	95
				I versus B	90
5b		60 versus 10 min 60 min versus fleeting 10 min versus fleeting		D versus H	<50
				D versus I	60
				H versus I	50

For each parameter described, the two average S/N values from a pair of data groups were tested for distinctness using statistical *T* tests as described in the experimental section and Appendix 2. A high confidence level for a pair of data groups suggests that the two groups are very likely statistically distinct from each other (e.g. comparisons 1 and 5a), while a low confidence level suggests that they are not (e.g. comparisons 4b and 5b), signifying that the experimental variable in question is or is not relevant to PCR output, respectively

from each other. Comparison 3 shows that, regarding CE injection plug formation time, a 90-s injection is preferable to a 60-s injection, likely due to a greater amount of the product front having arrived at the channel intersection (Footz et al. 2001) at the time of injection into the separation channel. This effect is no longer pronounced when a sample stacking solution is used prior to injection, as discussed next (dilution 1 for data groups M vs. L). Comparisons 4a and b regarding CE sample preparation show that dilution with a low ionic strength buffer ($0.1\times$ or $0.01\times$ TTE for dilution 1 or 2, respectively) to promote sample stacking did seem to produce an improvement for 60-s injections (comparison 4a, data groups L and N vs. J, respectively), but not for 90-s injections (comparison 4b, data groups G vs. D and M vs. K, respectively). Also, no appreciable improvement was seen moving from $0.1\times$ to $0.01\times$ TTE stacking solutions (comparison 4a, data groups N vs. L). Comparisons 5a and b show that any BSA pre-soak duration, whether fleeting (just prior to PCR), 10 or 60 min, confers a substantial output benefit to the PCR (comparison 5a), but that the benefit does not appear to increase with longer soak times (comparison 5b). The conclusion of comparison 5a that static BSA passivation (i.e. imparted by a pre-coating) improves upon the dynamic

BSA passivation (i.e. imparted by inclusion in PCR reagent mixture) we achieve without a pre-coat is in agreement with the results of Xia et al. (2007) using PEG and PVP. Though dynamic BSA passivation alone is insufficient to generate detectable product in our experience, it has been successfully used by others to enhance PCR output aboard non-PDMS microfluidic devices (Taylor et al. 1997; Giordano et al. 2001; Erill et al. 2003; Hataoka et al. 2005; Oh et al. 2005; Chen et al. 2005; Cheng et al. 2005; Cho et al. 2006; Dunn et al. 2000; Felbel 2002; Gong et al. 2006; Hashimoto et al. 2006; Lee et al. 2006; Liu et al. 2002a, b; Panaro et al. 2005; Shen et al. 2005; Trau et al. 2002) or, more rarely, aboard PDMS devices without a static coating (Liu et al. 2006; Nakayama et al. 2006; Zhang et al. 2010). Two groups performing PCR aboard PDMS devices make no mention of either inhibition or passivation (Liu et al. 2002a, b, 2008). In summary, there is not good agreement in the literature as to the necessity or superiority of static versus dynamic BSA coatings. Also, there is a wide variety of BSA concentrations used for either type of coating; our 1 % concentration was adopted from other research (Matsubara et al. 2005; Cady et al. 2005; Koh et al. 2003). Lastly, though not shown in either Table 4 or 5, we did track changes in reagent lots for

PDMS (and other) reagents during the course of our investigation, but were not able to attribute any changes in PCR performance to a change in reagent lot.

The single most obvious trend that is evident from Tables 4 and 5 is the effectiveness of BSA in improving PCR product peak signal strength (comparisons 1 and 5a). In the three direct comparison cases, the average S/N enhancement factors were 10 \times , 23 \times and 40 \times (comparison 1 data groups C vs. A, D vs. B and G vs. F, respectively), and for all but one non-BSA pre-coated case (run ID 65), the S/N values were below the limit of quantitation (<10). While we cannot be sure of the mechanisms that act to inhibit PCR in uncoated (and, to a lesser degree, coated) chips, it is plausible to imagine that a BSA coating on the glass and PDMS channel surfaces can reduce the loss or fouling of polymerase or other reactants via any or all of (1) adsorption on the glass or PDMS surfaces, (2) absorption within the porous PDMS polymer network or (3) release of leachates from the PDMS (or glass) into the liquid reaction matrix. A recent study (Schrott et al. 2009) quantified the extent of BSA coverage on PDMS surfaces in microfluidic channels, after using a pre-coating procedure very similar to ours (1 % BSA for 10 min), and estimated that only 40 % of the surface was covered based on electroosmotic mobility and atomic force microscopy measurements. The extent of uncoated area (and consequent inhibition by adsorption) within our BSA-coated chip is not known. We and other researchers are experimenting with parylene (Chen et al. 2009; Shin et al. 2003), paraffin wax (Ren et al. 2010) and other coating options in the hopes of finding a bio-compatible approach which is at once effective at reproducibly enhancing PCR yield, and manufacturable with ease and low cost.

4 Conclusions

As the development of microfluidic devices progresses to greater and greater levels of functional integration, new challenges arise from unwanted surface chemistry interactions at the reduced size scale implicit in miniaturisation. In keeping with the work of several other researchers, our work shows that, in a high SA:V miniaturised device, the immediate environment for PCR can dramatically inhibit its output. While our chip-flush findings do not provide irrefutable evidence of any particular mechanism for PCR inhibition, they are consistent with and suggestive of one or likely several postulated mechanisms of polymerase or other reagent fouling: adsorption and/or absorption to PDMS or glass surfaces in chip channels, and contaminant leaching from PDMS.

We have also shown that, for PCR–CE performed in a microfluidic hybrid PDMS–glass environment, BSA

pre-coating of the PCR channel network provides a critical 10–40 \times enhancement in signal-to-noise of the product peak, raising the level from below the limits of detection or quantitation to easily detectable for raw data. The pre-coating procedure is simple and effective, and may lead to other surface treatment options that can be incorporated into chip manufacture.

The need to address surface biocompatibility issues for on-chip PCR and other bio-sample manipulations represents a significant challenge for the development of microfluidics devices targeted for biological diagnostics. A significant issue is the need to test many different chips, not just a few, empirically chosen for their ability to provide an optimal PCR environment. Many of our (and perhaps others') early proof-of-principle studies made use of a small number of effective devices which did not reveal reliability issues. However when, as in this study, a large number of chips are tested, the inhibitory effects become more apparent, seriously compromising the reliability of on-chip PCR.

A chip design, fabrication process and operation protocol are required to provide a high yield of consistently reliable chips for PCR. Several approaches to improve on-chip PCR output can be considered. (1) In a device that incorporates PDMS membrane valving, incorporation of an additional glass layer will dramatically reduce the exposure of the PCR reagents to the membrane. This was pioneered by the Mathies group, and ostensibly provides the isolation required at the price of device complexity. (2) The use of effective coatings, as in this study, can reduce unwanted surface interactions. In comparison to the additional glass (or inert) layer approach, this approach confers a reduction in device complexity and hence cost, but will require development for ease of manufacturability. (3) Generation of fluid control via off-chip pumping and valving, where SA:V ratios are far lower. Properly chosen device and instrument materials may all but eliminate the surface chemistry problem, but transfer the need for miniaturised integrated components from the chip to the instrument. The disadvantages may be increased cost and reduced performance owing to larger reagent quantities and dead volumes. (4) Finally, use of a pseudo-solid matrix that limits diffusion can reduce surface chemistry interactions between reagents and the device channel network walls. We have begun experimentation in this area (Atrazhev et al. 2010) using a gel matrix with discrete reaction elements that bypass problems associated with surface chemistry by isolating the PCR from the glass, PDMS or other device materials.

Acknowledgments We thank Dr. Xiao-Li Pang at the Alberta Provincial Laboratory for Public Health in Edmonton for kindly providing BKV samples for this study. We also thank Dr. Eric Lagally at Lagally Consulting and Dr. Will Grover at the Massachusetts Institute of Technology for their valuable advice. Micralyne Inc. is gratefully

acknowledged for the donation of glass microfluidic chips. This research was funded by the Alberta Heritage Foundation for Medical Research's Interdisciplinary Team Grants Program.

Appendix 1

Product peak quantitation, described briefly previously, is described next in more detail and illustrated in Fig. 2. Plot A of Fig. 2 shows a typical electropherogram for the PCR output, with a peak for each of the primer and product peaks; plot B shows the area of interest for S/N calculations at and before the product peak for an on-scale peak; plot C shows the same as plot B but for an off-scale product peak; and plot D shows a magnification of the baseline segment used to determine both peak height and magnitude of noise. After manually bracketing the time window for each product peak, all data processing was automated using Microsoft Excel 2003 or 2010 spreadsheet functions to remove human bias. Electropherogram data were loaded in Excel directly from the μ TK exported text files without smoothing or alteration. For each electropherogram, the product peak maximum was located, and 2 s of baseline data, from 7 to 5 s before the peak maximum, was used to determine the baseline DC and noise magnitude (standard deviation or σ) values. Because the baseline was sloping down from the primer peak tail, the 2 s of baseline data was regressed linearly and the slope subtracted to produce 'corrected baseline' data (Fig. 2d). The DC value of this zero-slope corrected baseline was set to match the value at 5 s before the peak maximum, i.e. the data at 7 s before the peak were corrected (lowered) the most, while that at 5 s before was not corrected at all. The signal was calculated as the height difference between the peak maximum and corrected baseline, while the noise was calculated as the standard deviation of the corrected baseline.

In many instances, strong signal produced off-scale electrophoretic peaks. For these peaks, dual calculations were performed to generate both minimum and estimated S/N values based on minimum and estimated signal values (noise values were as described above). The minimum signal value was as described above, where the clipped peak maximum value (5 V) was used to calculate the peak's understated signal value. The estimated signal value was determined as the difference between the corrected baseline and the interpolated peak maximum. The interpolated peak maximum was calculated as 84.1 % of the height from the corrected baseline to the intersection of linear extrapolations of the clipped peak's front and tail. The peak's front and tail were linearly regressed from 65 to 95 % of on-scale peak height to reduce the impact of product peak tailing on the signal estimate. Additionally, a reducing factor (0.841) was required to account for the fact

that peaks are nominally Gaussian in nature, not triangular, and thus the extrapolation intersection just described is an over estimate of the peak maximum. The 84.1 % fraction is the height of an ideal Gaussian peak relative to the height determined by the method above: the intersection of linear extrapolations (from 40 to 60 % of peak height) of the peak's front and tail (data not shown). Comparison of this graphically interpolated estimate of peak height to actual peak heights for on-scale peaks showed the interpolated values to be conservative in all cases.

Appendix 2

The statistical approach (Snedecor and Cochran 1980) used to evaluate the distinctness of averages in a comparison of Table 3 data groups, some of small sample size and most highly variable, is described next. We wish to determine whether two average S/N values, A and B, with corresponding standard deviations s_A and s_B and sample sizes N_A and N_B , are statistically different from each other at a chosen confidence level (CL), assuming a normal (Gaussian) distribution of errors. If they are distinct from each other at that CL, then the following inequality applies:

$$|A - B| > t_{CL,DF} \times \sqrt{\frac{s_A^2}{N_A} + \frac{s_B^2}{N_B}} \quad (1)$$

where $t_{CL,DF}$ is the Student's t value for the chosen two-sided CL and number of degrees of freedom, DF, for the difference between the two averages. The latter is evaluated as:

$$DF = \frac{\left(\frac{s_A^2}{N_A} + \frac{s_B^2}{N_B}\right)^2}{\frac{\left(\frac{s_A^2}{N_A}\right)^2}{(N_A - 1)} + \frac{\left(\frac{s_B^2}{N_B}\right)^2}{(N_B - 1)}} \quad (2)$$

where DF is rounded down to the nearest integer value.

In practice, we evaluated all the data group comparisons shown in Table 4 at each confidence level (50, 60, 70, 80, 90, 95, 98, 99, 99.5, 99.8 and 99.9 %), and reported the highest CL for which A and B could be considered distinct per Eq. (1) as a measure of the strength of the distinction.

References

- Atrazhev A, Manage DP, Stickel AJ et al (2010) In-gel technology for PCR genotyping and pathogen detection. *Anal Chem* 82:8079–8087
- Berdichevsky Y, Khandurina J, Guttman A, Lo Y-H (2004) UV/ozone modification of poly(dimethylsiloxane) microfluidic channels. *Sens Actuators B Chem* 97:402–408

- Beyor N, Yi L, Seo T, Mathies R (2009) Integrated capture, concentration, polymerase chain reaction, and capillary electrophoretic analysis of pathogens on a chip. *Anal Chem* 81:3523–3528
- Bontoux N, Dauphinot L, Vitalis T et al (2008) Integrating whole transcriptome assays on a lab-on-a-chip for single cell gene profiling. *Lab Chip* 8:443
- Cady NC, Stelick S, Kunnavakkam MV, Batt CA (2005) Real-time PCR detection of *Listeria monocytogenes* using an integrated microfluidics platform. *Sens Actuators B Chem* 107:332–341
- Chen Z, Wang J, Qian S, Bau H (2005) Thermally-actuated, phase change flow control for microfluidic systems. *Lab Chip* 5: 1277–1285
- Chen M, Huang H, Pierstorff E et al (2009) Parylene-encapsulated copolymeric membranes as localized and sustained drug delivery platforms. *Ann Biomed Eng* 37:2003–2017
- Cheng J, Hsieh C, Chuang Y, Hsieh J (2005) Performing microchannel temperature cycling reactions using reciprocating reagent shuttling along a radial temperature gradient. *Analyst* 130:931–940
- Cho Y, Kim J, Lee Y et al (2006) Clinical evaluation of micro-scale chip-based PCR system for rapid detection of hepatitis B virus. *Biosens Bioelectron* 21:2161–2169
- Chou Q, Russell M, Birch DE et al (1992) Prevention of pre-PCR mis-priming and primer dimerization improves low-copy-number amplifications. *Nucleic Acids Res* 20:1717–1723
- Christensen T, Pedersen C, Grondhal K et al (2007) PCR biocompatibility of lab-on-a-chip and MEMS materials. *J Micromech Microeng* 17:1527–1532
- Crabtree HJ, Cheong ECS, Tilroe DA, Backhouse CJ (2001) Microchip injection and separation anomalies due to pressure effects. *Anal Chem* 73:4079–4086
- D'Aquila RT, Bechtel LJ, Videler JA et al (1991) Maximizing sensitivity and specificity of PCR by preamplification heating. *Nucleic Acids Res* 19:3749
- Dunn WC, Jacobson SC, Waters LC et al (2000) PCR amplification and analysis of simple sequence length polymorphisms in mouse DNA using a single microchip device. *Anal Biochem* 277: 157–160
- Efimenko K, Wallace WE, Genzer J (2002) Surface modification of Sylgard-184 poly(dimethyl siloxane) networks by ultraviolet and ultraviolet/ozone treatment. *J Colloid Interface Sci* 254:306–315
- Erill I, Campoy S, Erill N et al (2003) Biochemical analysis and optimization of inhibition and adsorption phenomena in glass-silicon PCR-chips. *Sens Actuators B Chem* 96:685–692
- Felbel J (2002) Chemical surface management for micro PCR in silicon chip thermocyclers. *SPIE Biomed Appl Micro Nanoeng* 2002:34–40
- Footz T, Wunsam S, Kulak S et al (2001) Sample purification on a microfluidic device. *Electrophoresis* 22:3868–3875
- Fraga D, Meulia T, Fenster S (2008) Real-time PCR. *Curr Protoc Essential Lab Tech* 1:10.3.1–10.3.34
- Giordano BC, Copeland ER, Landers JP (2001) Towards dynamic coating of glass microchip chambers for amplifying DNA via the polymerase chain reaction. *Electrophoresis* 22:334–340
- Gong H, Ramalingam N, Chen L et al (2006) Microfluidic handling of PCR solution and DNA amplification on a reaction chamber array biochip. *Biomed Microdevices* 8:167–176
- Gonzalez A, Grimes R, Walsh E et al (2007) Interaction of quantitative PCR components with polymeric surfaces. *Biomed Microdevices* 9:261–266
- Grover W, Skelley A, Liu C et al (2003) Monolithic membrane valves and diaphragm pumps for practical large-scale integration into glass microfluidic devices. *Sens Actuators B Chem* 89:315–323
- Hashimoto M, Barany F, Soper S (2006) Polymerase chain reaction/ligase detection reaction/hybridization assays using flow-through microfluidic devices for the detection of low-abundant DNA point mutations. *Biosens Bioelectron* 21:1915–1923
- Hataoka Y, Zhang L, Yukimasa T, Baba Y (2005) Rapid microvolume PCR of DNA confirmed by microchip electrophoresis. *Anal Sci* 21:53–56
- Heo Y, Cabrera L, Song J et al (2007) Characterization and resolution of evaporation-mediated osmolality shifts that constrain microfluidic cell culture in poly(dimethylsiloxane) devices. *Anal Chem* 79:1126–1134
- Hoang V, Kaigala G, Atrazhev A et al (2008) Strategies for enhancing the speed and integration of microchip genetic amplification. *Electrophoresis* 29:4684–4694
- Kaigala GV, Huskins RJ, Preiksaitis J et al (2006) Automated screening using microfluidic chip-based PCR and product detection to assess risk of BK virus-associated nephropathy in renal transplant recipients. *Electrophoresis* 27:3753–3763
- Kaigala G, Hoang V, Stickel A et al (2008) An inexpensive and portable microchip-based platform for integrated RT-PCR and capillary electrophoresis. *Analyst* 133:331–338
- Kaigala GV, Behnam M, Bidulock ACE et al (2010) A scalable and modular lab-on-a-chip genetic analysis instrument. *Analyst* 135: 1606–1617
- Koh CG, Tan W, Zhao M et al (2003) Integrating polymerase chain reaction, valving, and electrophoresis in a plastic device for bacterial detection. *Anal Chem* 75:4591–4598
- Kolari K, Satokari R, Kataja K et al (2008) Real-time analysis of PCR inhibition on microfluidic materials. *Sens Actuators B Chem* 128:442–449
- Kopp MU, Mello AJ, Manz A (1998) Chemical amplification: continuous-flow PCR on a chip. *Science* 280:1046–1048
- Kricka LJ, Wilding P (2003) Microchip PCR. *Anal Bioanal Chem* 377:820–825
- Lagally ET, Simpson PC, Mathies RA (2000) Monolithic integrated microfluidic DNA amplification and capillary electrophoresis analysis system. *Sens Actuators B Chem* 63:138–146
- Lagally ET, Emrich CA, Mathies RA (2001a) Fully integrated PCR-capillary electrophoresis microsystem for DNA analysis. *Lab Chip* 1:102–107
- Lagally ET, Medintz I, Mathies RA (2001b) Single-molecule DNA amplification and analysis in an integrated microfluidic device. *Anal Chem* 73:565–570
- Lagally E, Scherer J, Blazej R et al (2004) Integrated portable genetic analysis microsystem for pathogen/infectious disease detection. *Anal Chem* 76:3162–3170
- Lee JN, Park C, Whitesides GM (2003) Solvent compatibility of poly(dimethylsiloxane)-based microfluidic devices. *Anal Chem* 75:6544–6554
- Lee J, Cheong K, Huh N et al (2006) Microchip-based one step DNA extraction and real-time PCR in one chamber for rapid pathogen identification. *Lab Chip* 6:886–895
- Liu J, Enzelberger M, Quake S (2002a) A nanoliter rotary device for polymerase chain reaction. *Electrophoresis* 23:1531–1536
- Liu Y, Rauch CB, Stevens RL et al (2002b) DNA amplification and hybridization assays in integrated plastic monolithic devices. *Anal Chem* 74:3063–3070
- Liu CN, Toriello NM, Mathies RA (2006) Multichannel PCR-CE microdevice for genetic analysis. *Anal Chem* 78:5474–5479
- Liu P, Seo TS, Beyor N et al (2007) Integrated portable polymerase chain reaction-capillary electrophoresis microsystem for rapid forensic short tandem repeat typing. *Anal Chem* 79:1881–1889
- Liu L, Cao W, Wu J et al (2008) Design and integration of an all-in-one biomicrofluidic chip. *Biomicrofluidics* 2:034103
- Manage D, Morrissey Y, Stickel A et al (2011) On-chip PCR amplification of genomic and viral templates in unprocessed whole blood. *Microfluid Nanofluid* 10:697–702
- Matsubara Y, Kerman K, Kobayashi M et al (2005) Microchamber array based DNA quantification and specific sequence detection

- from a single copy via PCR in nanoliter volumes. *Biosens Bioelectron* 20:1482–1490
- Mehta G, Lee J, Cha W et al (2009) Hard top soft bottom microfluidic devices for cell culture and chemical analysis. *Anal Chem* 81:3714–3722
- Nakayama T, Kurosawa Y, Furui S et al (2006) Circumventing air bubbles in microfluidic systems and quantitative continuous-flow PCR applications. *Anal Bioanal Chem* 386:1327–1333. doi:10.1007/s00216-006-0688-7
- Oh K, Park C, Namkoong K et al (2005) World-to-chip microfluidic interface with built-in valves for multichamber chip-based PCR assays. *Lab Chip* 5:845–850
- Ostuni E, Chen C, Ingber D, Whitesides G (2001) Selective deposition of proteins and cells in arrays of microwells. *Langmuir* 17:2828–2834
- Panaro N, Lou X, Fortina P et al (2005) Micropillar array chip for integrated white blood cell isolation and PCR. *Biomol Eng* 21:157–162
- Pilarski L, Lauzon J, Strachan E et al (2005) Sensitive detection using microfluidics technology of single cell PCR products from high and low abundance IgH VDJ templates in multiple myeloma. *J Immunol Methods* 305:94–105
- Prakash AR, Amrein M, Kaler KVIS (2007) Characteristics and impact of Taq enzyme adsorption on surfaces in microfluidic devices. *Microfluid Nanofluid* 4:295–305
- Ren K, Zhao Y, Su J et al (2010) Convenient method for modifying poly(dimethylsiloxane) to be airtight and resistive against absorption of small molecules. *Anal Chem* 82:5965–5971
- Rothka J, Studd R, Tate K, Belder D (2011) Outgassing of silicone elastomers (Arlon Silicone Technologies—Process Guides); <http://www.arlonstd.com/Library/Guides/Outgassing%20of%20Silicone%20Elastomers.pdf>
- Schneegeß I, Köhler JM (2001) Flow through polymerase chain reactions in chip thermocyclers. *Rev Mol Biotechnol* 82:101–121
- Schrott W, Slouka Z, Cervenka P et al (2009) Study on surface properties of PDMS microfluidic chips treated with albumin. *Biomicrofluidics* 3:044101
- Shen K, Chen X, Guo M, Cheng J (2005) A microchip-based PCR device using flexible printed circuit technology. *Sens Actuator B Chem* 105:251–258
- Shin YS, Cho K, Lim SH et al (2003) PDMS-based micro PCR chip with Parylene coating. *J Micromech Microeng* 13:768–774
- Shoffner MA, Cheng J, Hvichia GE et al (1996) Chip PCR. I. Surface passivation of microfabricated silicon-glass chips for PCR. *Nucleic Acids Res* 24:375–379
- Snedecor GW, Cochran WG (1980) *Statistical methods*, 7th edn. The Iowa State University Press, Ames
- Taylor T, WinnDeen E, Picozza E et al (1997) Optimization of the performance of the polymerase chain reaction in silicon-based microstructures. *Nucleic Acids Res* 25:3164–3168
- Toepke MW, Beebe DJ (2006) PDMS absorption of small molecules and consequences in microfluidic applications. *Lab Chip* 6:1484
- Trau D, Lee TMH, Lao AIK et al (2002) Genotyping on a complementary metal oxide semiconductor silicon polymerase chain reaction chip with integrated DNA microarray. *Anal Chem* 74:3168–3173
- Trung NB, Saito M, Takabayashi H et al (2010) Multi-chamber PCR chip with simple liquid introduction utilizing the gas permeability of polydimethylsiloxane. *Sens Actuator B Chem* 149:284–290
- Unger M, Chou H, Thorsen T et al (2000) Monolithic microfabricated valves and pumps by multilayer soft lithography. *Science* 288:113–116
- Valasek MA, Repa JJ (2005) The power of real-time PCR. *Adv Physiol Educ* 29:151–159
- Waters LC, Jacobsen SC, Kroutchinina N et al (1998) Multiple sample PCR amplification and electrophoretic analysis on a microchip. *Anal Chem* 70:5172–5176
- Wilding P, Shoffner M, Cheng J et al (1995) Thermal cycling and surface passivation of micromachined devices for PCR. *Clin Chem* 41:1367
- Wilson IG (1997) Inhibition and facilitation of nucleic acid amplification. *Appl Environ Microbiol* 63:3741–3751
- Wong I, Ho C-M (2009) Surface molecular property modifications for poly(dimethylsiloxane) (PDMS) based microfluidic devices. *Microfluid Nanofluid* 7:291–306
- Woolley AT, Hadley D, Landre P et al (1996) Functional integration of PCR amplification and capillary electrophoresis in a microfabricated DNA analysis device. *Anal Chem* 68:4081–4086
- Xia Y, Hua Z, Srivannavit O et al (2007) Minimizing the surface effect of PDMS–glass microchip on polymerase chain reaction by dynamic polymer passivation. *J Chem Technol Biot* 82:33–38
- Xu Z-R, Wang X, Fan X-F, Wang J-H (2009) An extrusion fluidic driving method for continuous-flow polymerase chain reaction on a microfluidic chip. *Microchim Acta* 168:71–78
- Yu C, Liang W, Kuan I et al (2007) Fabrication and characterization of a flow-through PCR device with integrated chromium resistive heaters. *J Chin Inst Chem Eng* 38:333–339. doi:10.1016/j.jcice.2007.05.001
- Zhang Y, Ozdemir P (2009) Microfluidic DNA amplification: a review. *Anal Chim Acta* 638:115–125
- Zhang C, Xing D (2007) Miniaturized PCR chips for nucleic acid amplification and analysis: latest advances and future trends. *Nucleic Acids Res* 35:4223–4237
- Zhang C, Xu J, Ma W, Zheng W (2006) PCR microfluidic devices for DNA amplification. *Biotechnol Adv* 24:243–284
- Zhang Y, Park S, Yang S, Wang T-H (2010) An all-in-one microfluidic device for parallel DNA extraction and gene analysis. *Biomed Microdevices* 12:1043–1049